MEMSlab

Microsystems for a Better Future

Dynamic Mode AFM Measurement of CMUT Diaphragm Deflection Profile

Sazzadur Chowdhury
Department of Electrical and Computer Engineering
University of Windsor
Windsor, ON, N9B 3P4, Canada
e-mail: sazzadur@uwindsor.ca

University of Windsor

IARIA

Sazzadur Chowdhury Bio

- Sazzadur Chowdhury is a professor in the department of Electrical and Computer Engineering in the University of Windsor, Windsor, Ontario, Canada and is the director of the MEM lab in the University
- The MEMS Lab is dedicated to develop microsystems to provide advanced healthcare, automotive safety, and security
- His current research interest is in the areas of Microscale sensing and actuation, Solid state radars, Ultrasonic transducers, Microfabrication, and 3-D heterogeneous integration
- He was awarded 10 USA and Canadian patents in the areas of MEMS based ultrasonic transducers, radars, and heterogeneous integration
- He published 70 peer reviewed research papers

Abstract

- Atomic Force Microscopy (AFM) measurement results of the deflection shape of a Capacitive Micromachined Ultrasonic Transducer (CMUT) diaphragm has been presented
- The AFM measurements were carried out using the dynamic mode operation of an atomic force microscope (FlexAFM ™, Nanosurf AG)
- The measurement results were used to calculate the roughness parameters and construct the post fabricated zero bias 3D deflection shapes of the CMUT diaphragm
- The measured deflection shape of the CMUT diaphragm can be used to determine CMUT diaphragm physical properties, such as residual stress, to facilitate more accurate calibration

CMUT Operating Principle

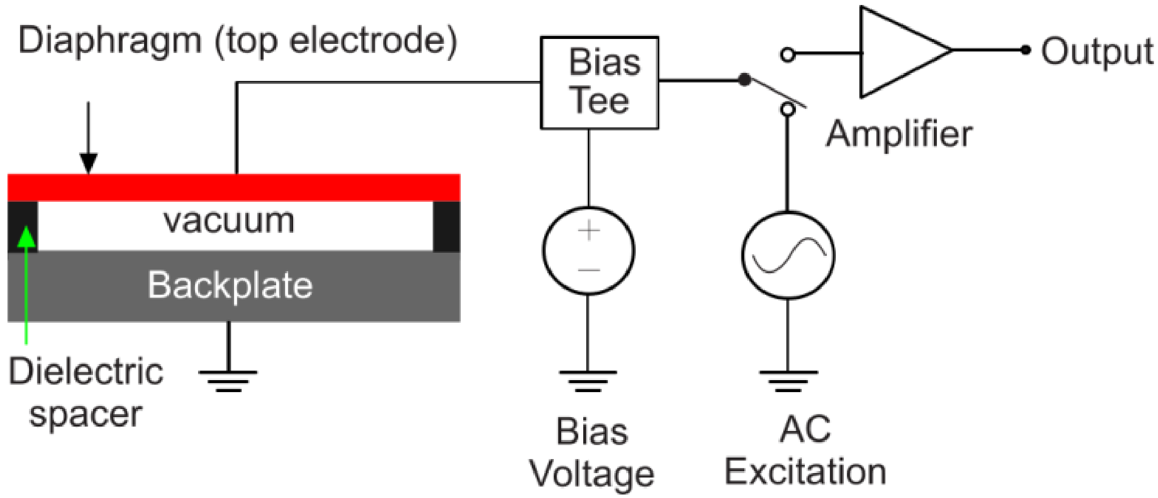

- A typical CMUT geometry is built to have a square or circular diaphragm separated from a fixed back plate by a small air gap or vacuum
- Basically, a variable capacitor
- When an AC voltage of desired frequency is superimposed in addition to the bias voltage, the diaphragm vibrates to generate ultrasound
- When the biased CMUT is exposed to an incoming ultrasound field, the diaphragm deforms to change the capacitance that generates a voltage
- A control circuit controls the switch to effect mode switching

CMUT Specifications

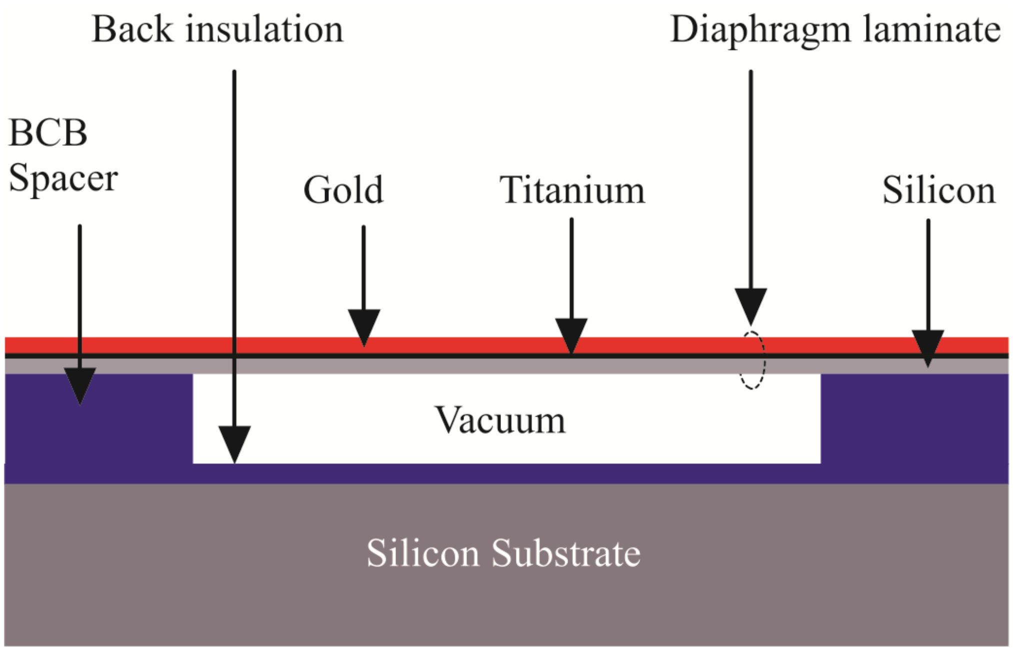

Measured CMUT Geometry

Parameter	Value	Unit
Diaphragm laminate thickness	800	nm
Gold layer thickness	100	nm
Silicon device layer thickness	700	nm
Cavity thickness	1	µm
Cavity width	28	µm
Sidewall width	10	µm
Bottom wafer thickness	500	µm

Fabricated CMUT Planar Array

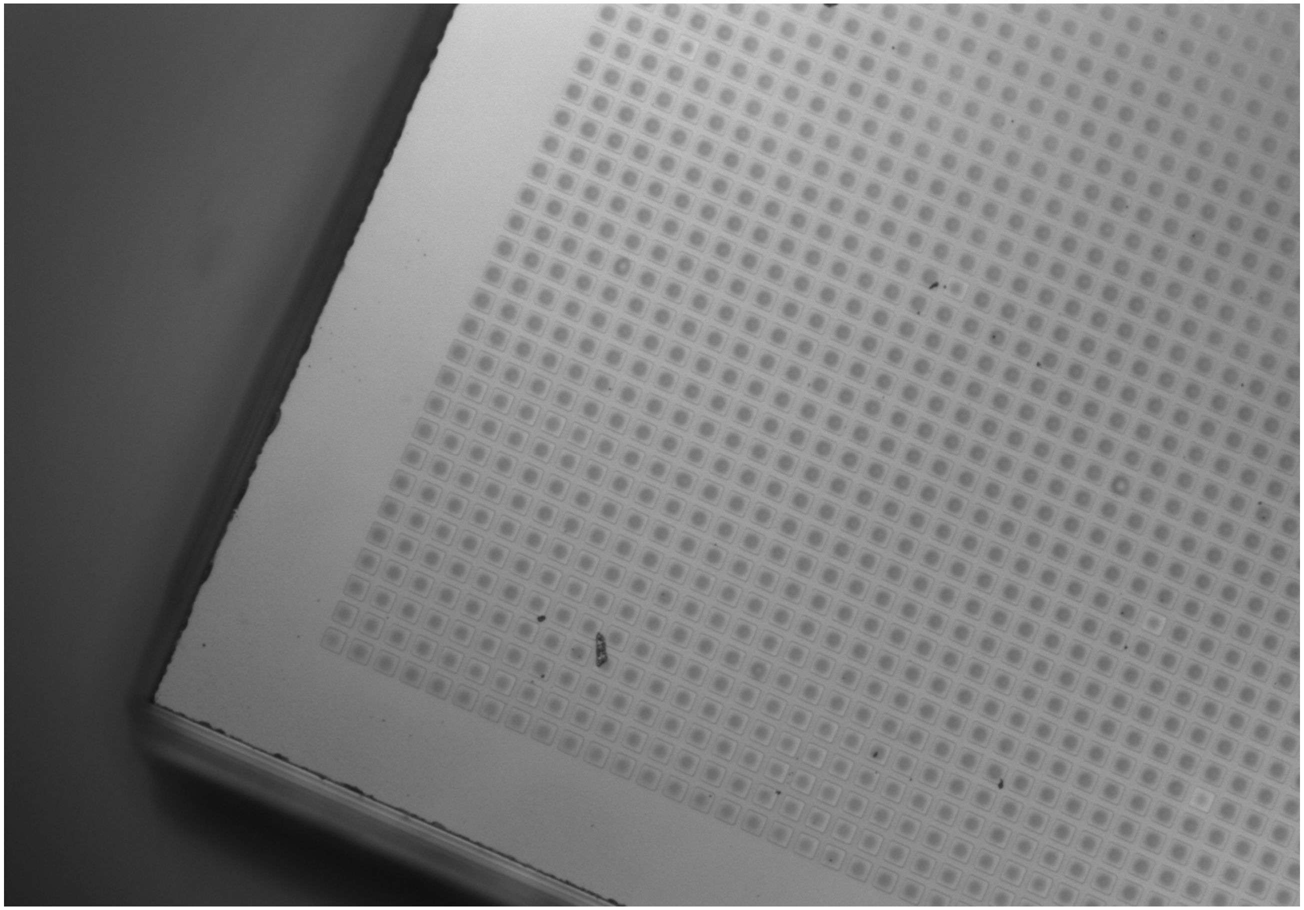

SEM image of the planar array

The array has 40 x 40 CMUT cells in a footprint area of 1870 x 1870 μm^2

AFM Dynamic Mode Operation

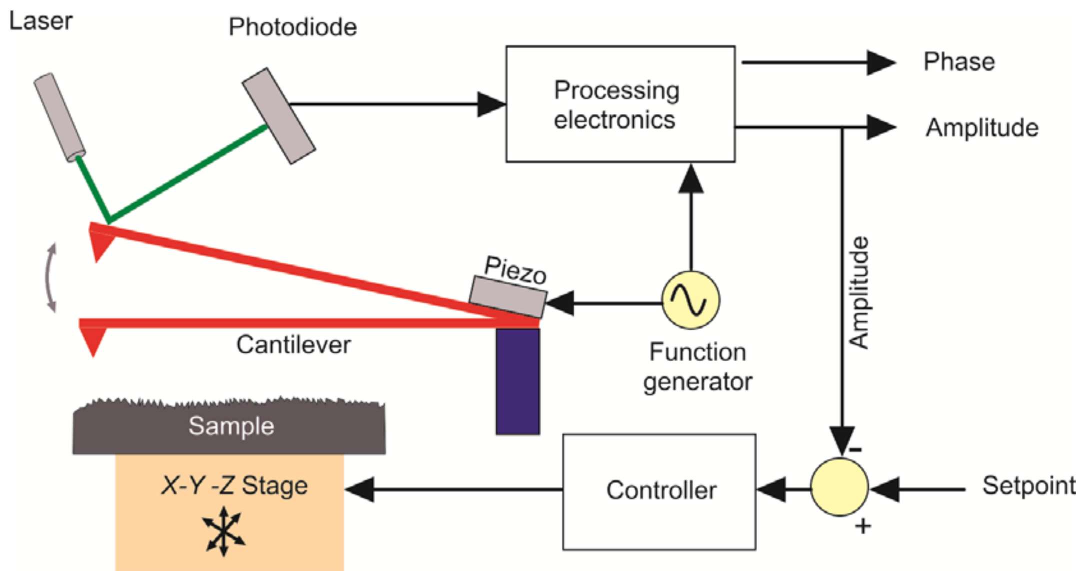

- An AFM technique creates a 3D topography of the sample's surface by scanning the surface using a sharp tip cantilever probe
- In the Dynamic Mode, the cantilever is forced to vibrate at its resonance frequency using a piezo element
- The vibration amplitude of the cantilever is detected using a laser and photodiode based detection system to use in a feedback loop
- The output of this feedback loop corresponds to the local sample height

Advantages of the Dynamic Mode

- The dynamic mode was chosen over the static mode due to the following reasons:

1. Gentle interaction of the probe tip with the surface improves accuracy
2. Minimized torsional forces between the probe and the sample, and
3. By using the cantilever’s oscillation amplitude as the feedback parameter, the user is able to fine-tune the interaction between probe and sample between different regimes- such as attractive and repulsive ones- to control the tip–surface distance on an atomic scale

- Better Control
- Higher Accuracy
- Higher Resolution

FlexAFM™ Data Processing Steps

Once the AFM measurement was done, the height data was processed following standard AFM data processing steps

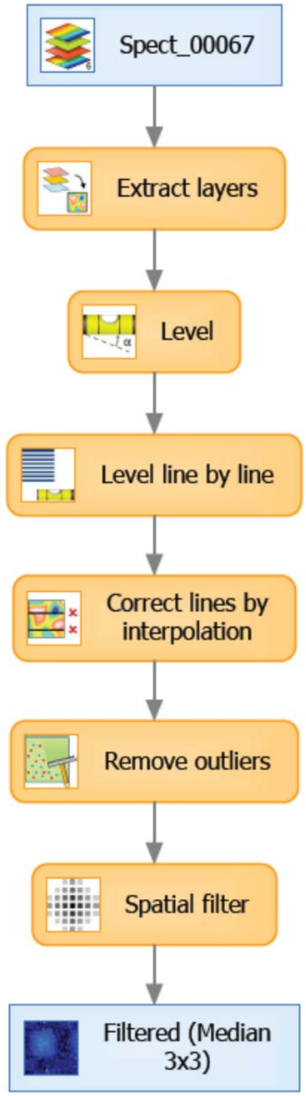

FlexAFM™

AFM Data for 3D Visualization

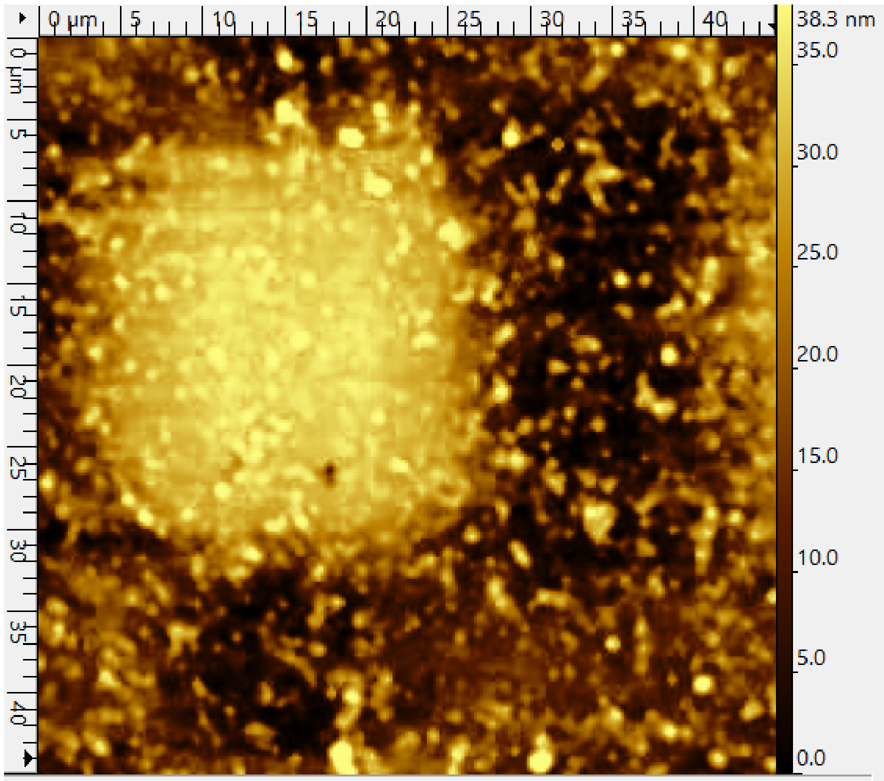

Pseudo-color view of the surface after processing

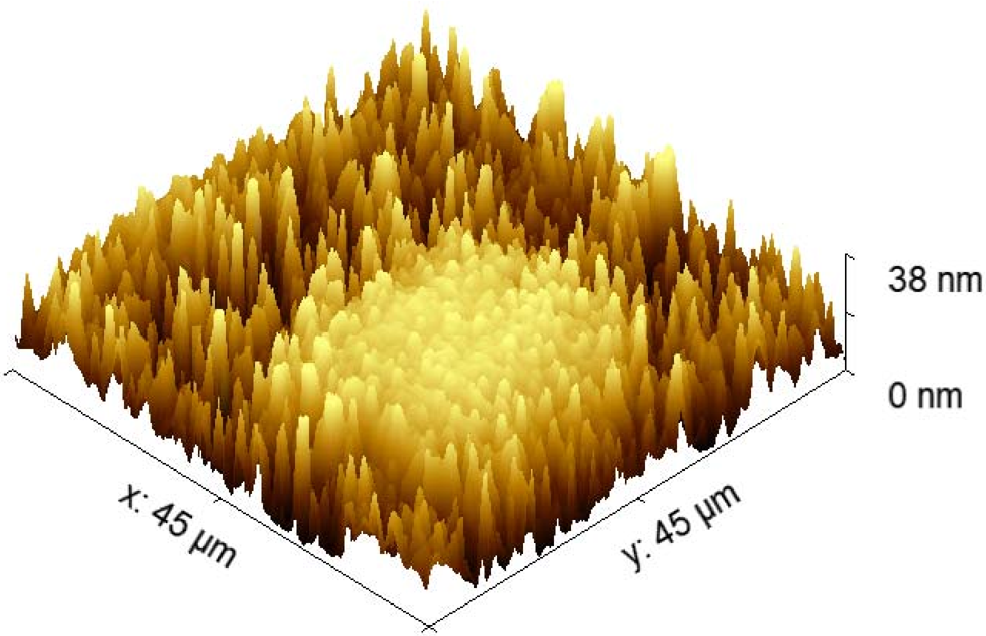

3-D height image in The Gwyddion™

IS0 25178 Roughness Parameters

The statistical roughness parameters following IS0 25178 have been determined using Gwyddion™

Parameter	Value	Unit
RMS roughness, S_q	10.50	nm
Mean-square roughness, S_a	9.08	nm
Skew, S_{sk}	0.06925	
Excess kurtosis	-1.185	
Maximum peak height, S_p	19.24	nm
Maximum pit depth, S_V	19.01	nm
Maximum height, S_z	38.25	nm
Projected area:	2025	μm^2
Surface area	2026	μm^2
Volume	38.50	μm^3

Surface vs Line Data

- AFM data are usually collected as line scans along the *x* axis
- x-axis data are concatenated together to form a 2-D image
- Scanning speed in the *x* direction is considerably higher than the scanning speed in the *y* direction
- As a result, the *x* profiles are less affected by low frequency noise and thermal drift of the sample as compared to the *y* profile
- Standardized one dimensional roughness parameters are considered more accurate

Line Scan Along *X* direction

One dimensional roughness parameters for a scan line centered approximately at the middle of the CMUT diaphragm along the y-axis

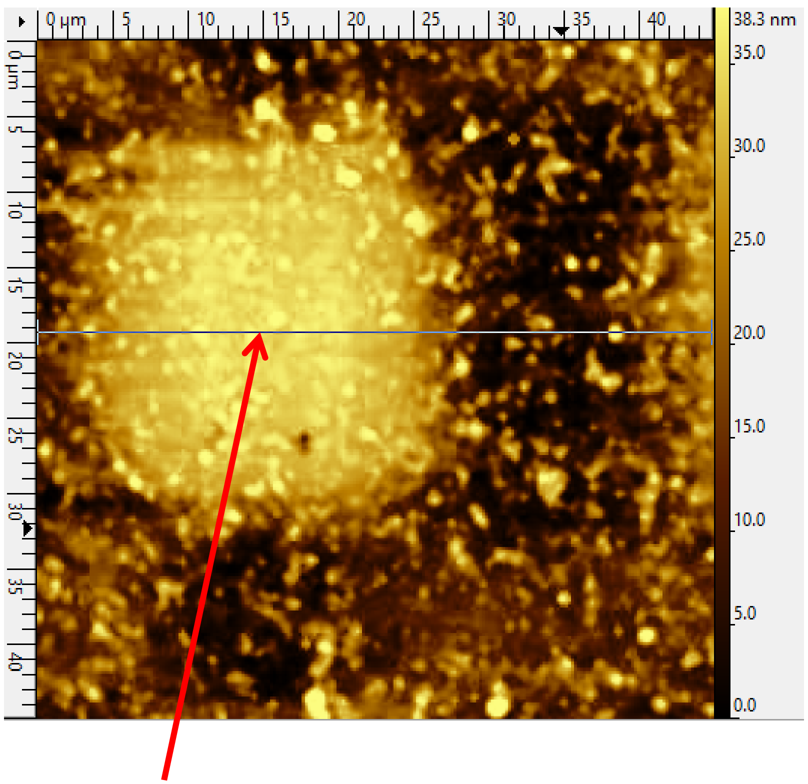

Scan line

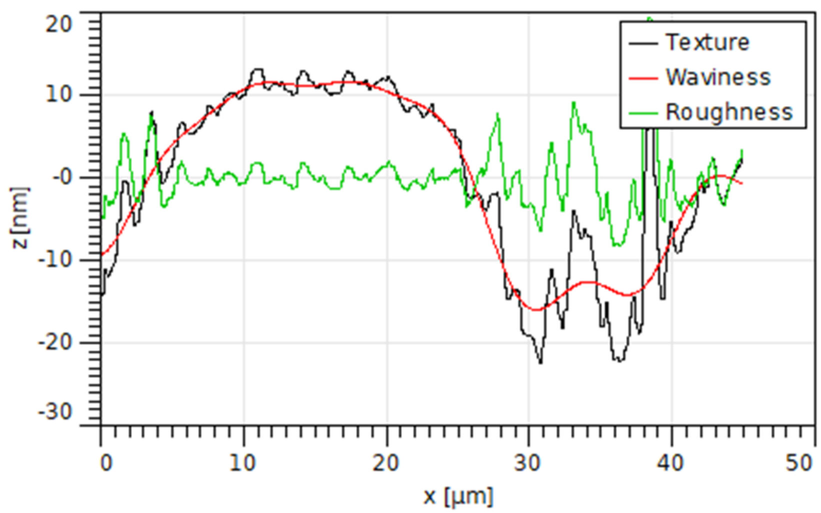

Roughness, texture, and waviness profile along the x- scan line

One Dimensional Roughness Parameters along the X Scan Line

Parameter	Value	Unit
Cut-off	7.69	µm
Roughness average, R_a	3.09	nm
Root mean square roughness, R_q	4.87	nm
Maximum height of the roughness, R_t	34.58	nm
Maximum roughness valley depth, R_v	10.67	nm
Maximum roughness peak height, R_p	23.91	nm
Average maximum height of the roughness, R_{tm}	17.92	nm
Average maximum roughness valley depth, R_{vm}	6.97	nm
Average maximum roughness peak height, R_{pm}	10.95	nm
Average maximum height of the profile, R_z	20.83	nm
Average maximum height of the roughness, R_z-ISO	17.92	nm
Waviness average, W_a	8.77	nm
Root mean square waviness, W_q	10.16	nm

Line Scan Along Y direction

One dimensional roughness parameters for a scan line centered approximately at the middle of the CMUT diaphragm along the x-axis

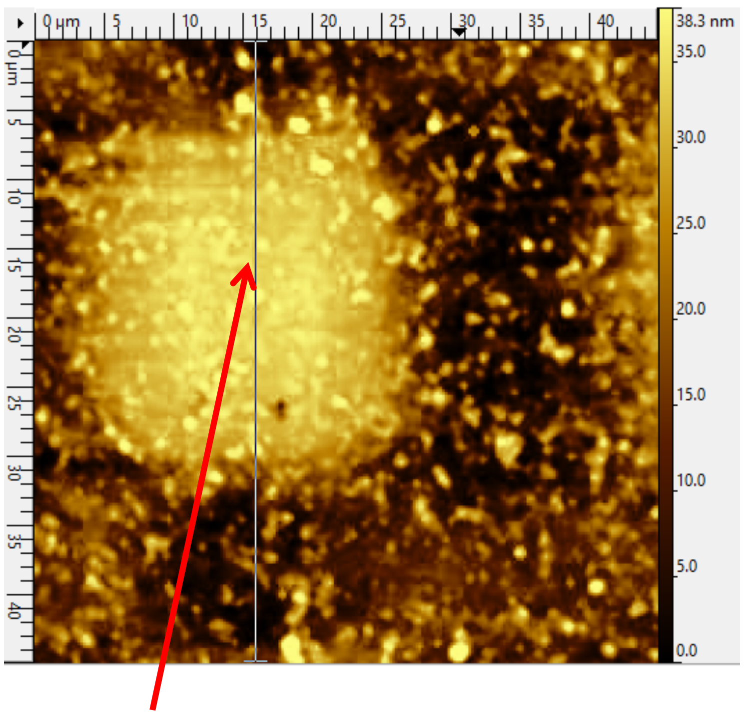

Scan line

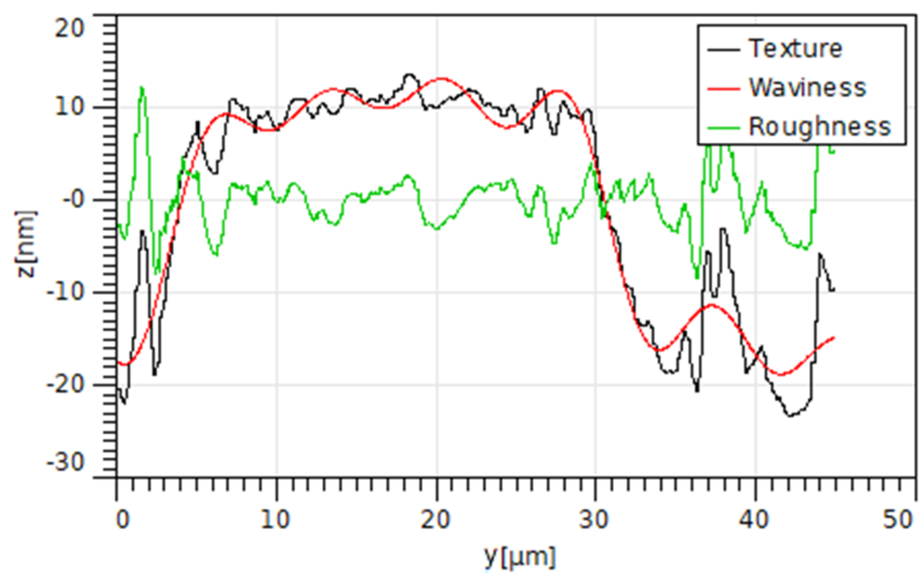

Roughness, texture, and waviness profile along the x- scan line

Line Scan Along An Arbitrary Direction

Arbitrary direction scan

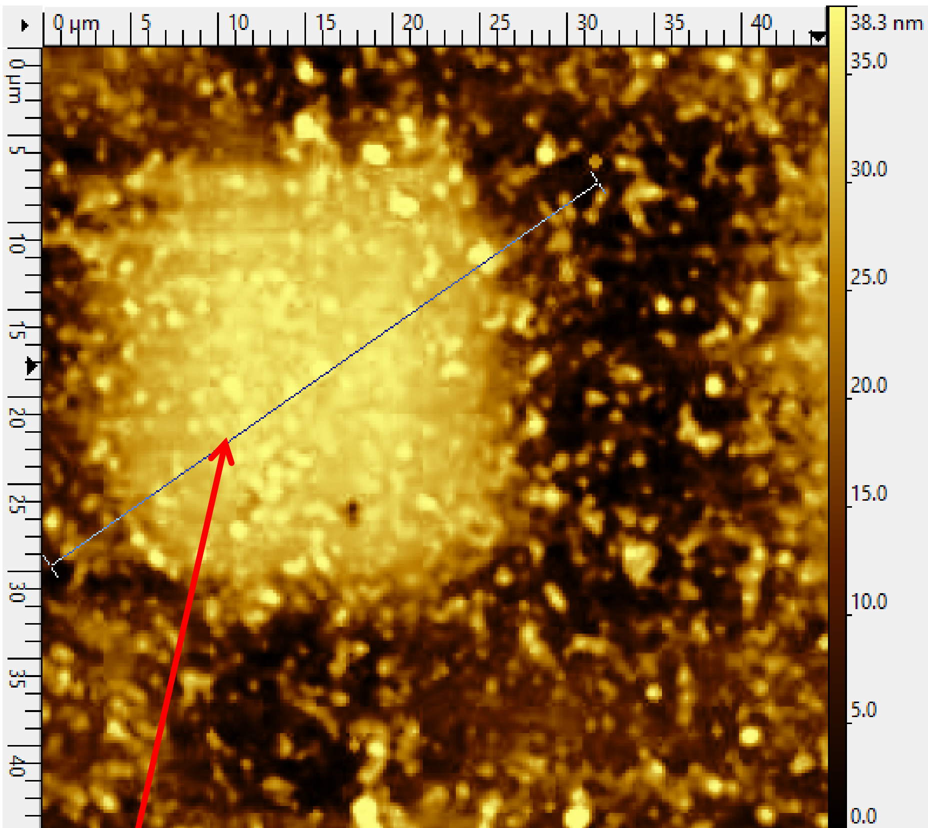

Scan line

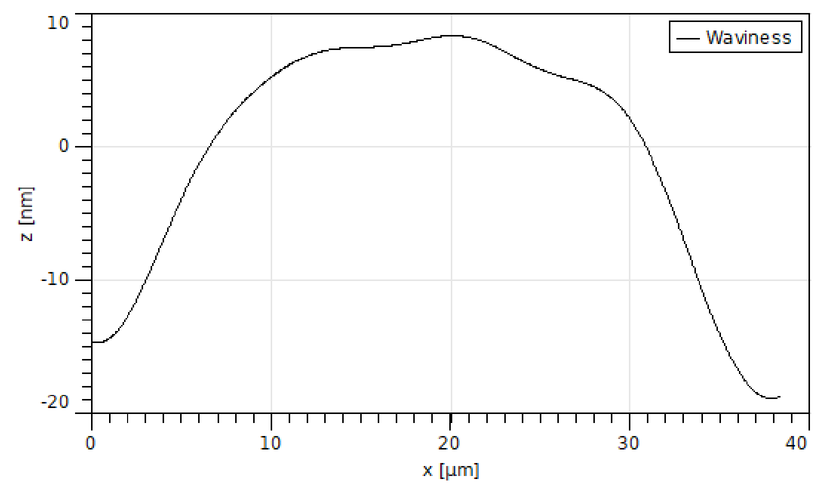

Waviness profile along the arbitrary scan line

High Frequency Filtering with a Gaussian Filter

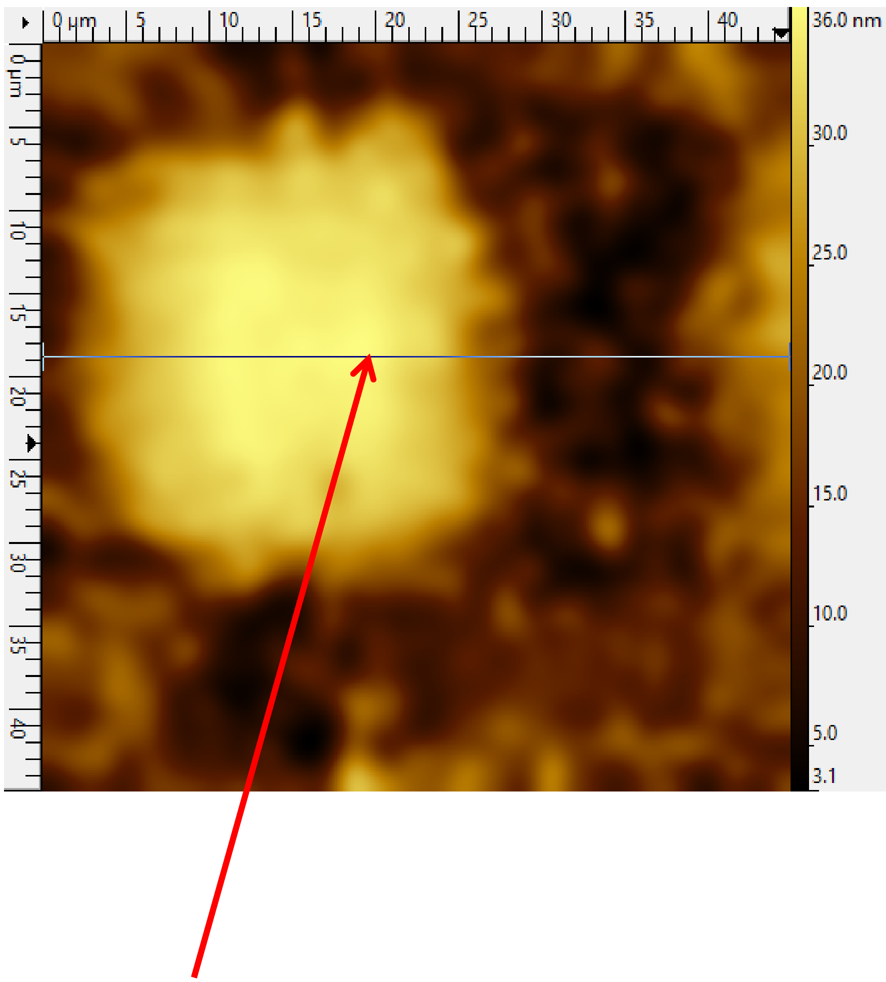

Scan line

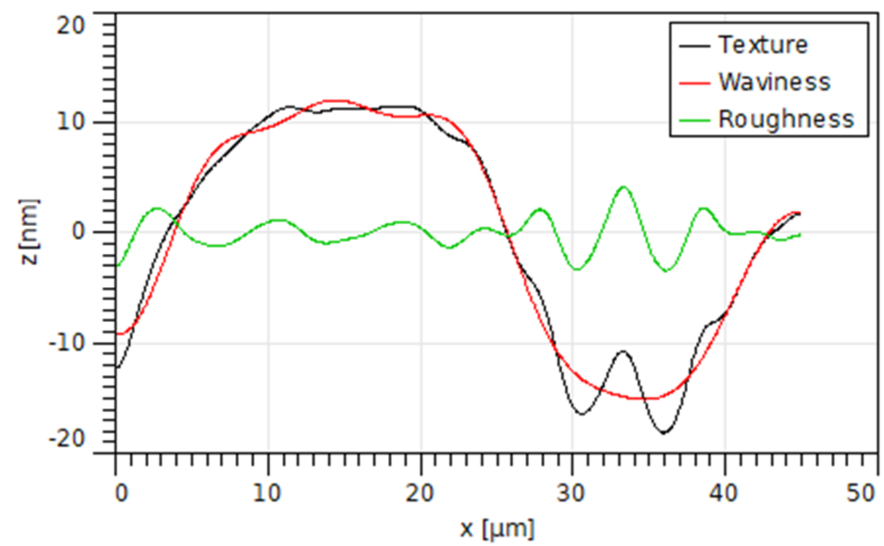

Roughness, texture, and waviness profile along the *x*-directional scan after applying a Gaussian filter

Waviness Measurement After High Frequency Filtering

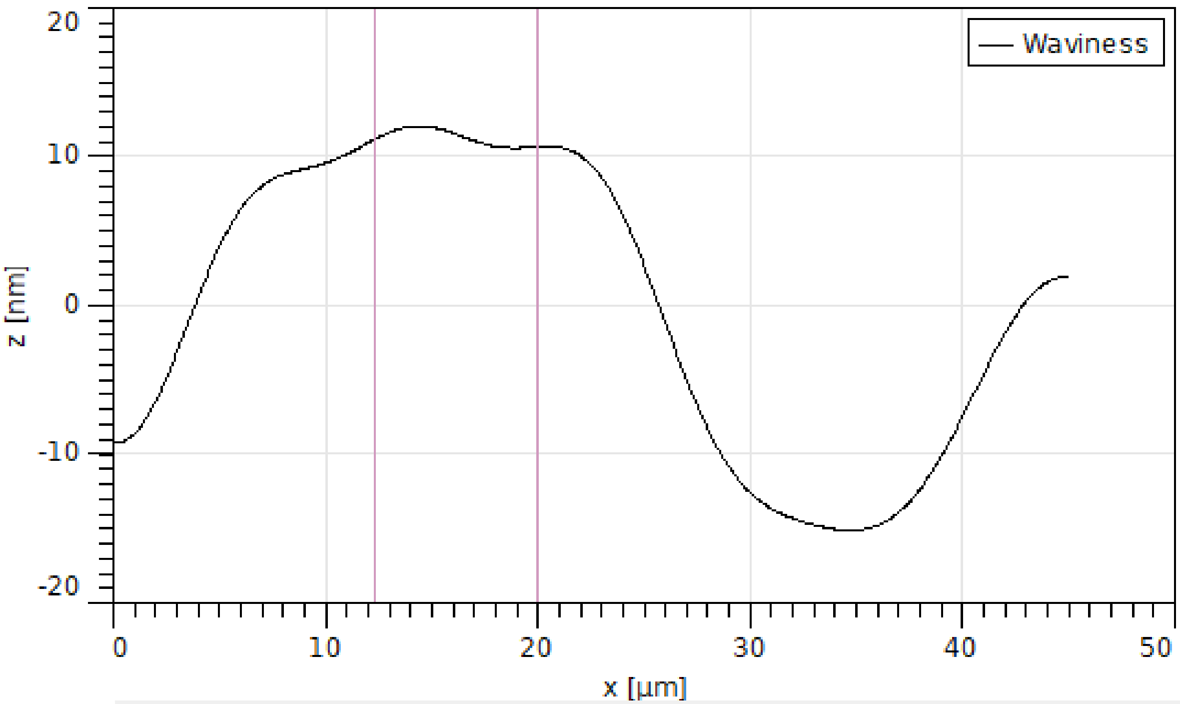

Points	X [µm]	Y [nm]	Length [µm]	Height [nm]	Angle [deg]
	12.32	11.18			
	19.98	10.67	7.66	-0.51	-0.00

Waviness profile measurement over a length on filtered data 7.66 micrometers (two red markers)

- The waviness average height is 8.85 nm
- Maximum height is 11.18 nm to 10.67 nm over this range
- Almost a flat surface

3D Top and Bottom View

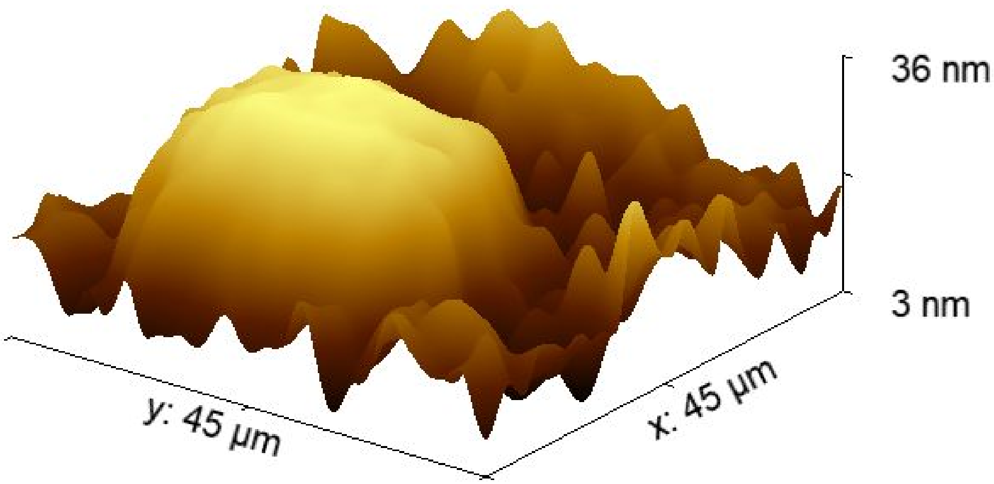

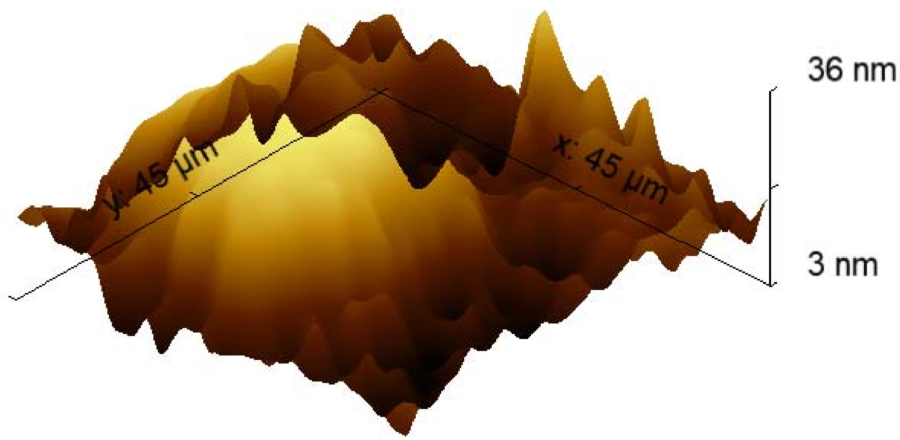

3D top and bottom views of the deflection profile after Gaussian filtering

Conclusions

- The presented dynamic mode AFM measurement and data analysis of a CMUT diaphragm appears to be a valuable method to evaluate the deflection profile of a CMUT diaphragm with a very high degree of accuracy
- Main advantage of the proposed method is that the height data is measured directly with nanometer scale precision instead of inferring from a 2D projection of an optical image
- Such deflection profiles can be used to determine the residual stress and other physical parameters of a CMUT diaphragm to aid in fine tuning of the process parameters to optimize CMUT diaphragm vibrational characteristics to obtain high quality images
- Additionally, the dynamic mode enables to measure the deflection shape of insulating materials, thus enabling to measure the diaphragm shapes where the diaphragm has an insulating top surface
- Overall, the dynamic mode AFM can provide high accuracy high resolution nanometer scale measurements to characterize CMUT surfaces

Thank You for Your Support

- Natural Sciences and Engineering Research Council of Canada (NSERC)
- Nanosurf AG, Switzerland
- CMC Microsystems, Canada
- IntelliSense Software Corporation of Woburn, MA., USA

References

[1] A. Ergun, G. Yaralioglu; and B. T. Khuri-Yakub, “Capacitive Micromachined Ultrasonic Transducers: Theory and Technology,” *Journal of Aerospace Engineering*, vol. 16, no. 2, pp. 76-84, Apr. 2003,

[2] B. T. Khuri-Yakub and Ö. Oralkan, “Capacitive Micromachined Ultrasonic Transducers for Medical Imaging and Therapy,” *Journal of Micromech .and Microeng*, vol. 21, no. 5, pp. 054004–054014, May, 2011.

[3] M. Klemm, “Acoustic Simulation and Characterization of Capacitive Micromachined Ultrasonic Transducers,” Ph.D. dissertation, Dresden University of Technology, TUD Press, Dresden, Germany, 2017.

[4] S. Berg, “Capacitive Micromachined Ultrasonic Transducers,” Ph.D. Dissertation, Dept. of Electronics and Telecommunications, Norwegian University of Science and Technology, Trondheim, Norway, 2012.

[5] E. Cianci, et al., “Fabrication Techniques in Micromachined Capacitive Ultrasonic Transducers and their Applications,” in MEMS/NEMS Handbook, Springer, Boston, MA, C. Leondes (eds), 2006, pp. 353-382.

[6] S. Savoia, G. Caliano, and M. Pappalardo, “A CMUT Probe for Medical Ultrasonography: From Microfabrication to System Integration,” *IEEE Transactions on Ultrasonics, Ferroelectrics, and Frequency Control*, vol. 59, no. 6, pp. 1127-1138, Jun.2012.

[7] A, Unamuno, "New Applications for Ultrasound Technology Through CMUTs," Fraunhofer IPMS, Presentations at the joint event MNBS 2013 and EPoSS general assembly annual forum 2013/eposs-annual-forum-2013-26-september-2013, [Online]. Available from: http://www.smart-systems-integration.org Accessed on: Oct. 5, 2020.

[8] M. Rahman, J. Hernandez, and S. Chowdhury, “An Improved Analytical Method to Design CMUTs with Square Diaphragms,” *IEEE Transactions on Ultrasonics, Ferroelectrics, and Frequency Control*,” vol. 60, no. 4, pp. 834-845, Apr. 2013.

[9] A. Bakhtazad and S. Chowdhury, “An evaluation of optical profilometry techniques for CMUT characterization,” *Microsystem Technologies*, Springer, vol. 25, pp. 3627-3642, Sep. 2019.

[10] Nanosurf AG, Switzerland, “Flex-Axiom The most flexible AFM for materials research,” [Online]. Available from: https://www.nanosurf.com/downloads/Nanosurf-Flex-Axiom-Brochure.pdf, Accessed on: Oct 2, 2020.

[11] L. Chaurette, N. Cheng, and B. Stuart, “Atomic Force Microscopy,” University of British Columbia, [Online]. Available from: https://phas.ubc.ca/~berciu/TEACHING/PHYS502/PROJECTS/AFM16.pdf, Accessed on: Oct 2, 2020.

[12] A. Bakhtazad, R. Manwar, and S. Chowdhury, “Fabrication and Characterization of Sealed Cavities Realized by Adhesive Wafer Bonding with Dry Etched Cyclotene,” *Microsystem Technologies*, Springer, vol. 21, issue 11, pp. 1-8, Jan. 2015.

[13] Biomedical Engineering Reference In-Depth Information, “Atomic Force Microscopy, “ [Online]. Available from: http://what-when-how.com/Tutorial/topic- 55iija/Atomic-Force-Microscopy-10.html, Accessed on: Sep. 4, 2020.

[14] Park Systems, “How AFM Woks, [Online]. Available from: https://parksystems.com/medias/nano-academy/how-afm-works, Accessed on: Oct. 4, 2020.

[15] C. Serra-Rodríguez, Re: Can we compare average roughness values obtained from AFM and Optical Profilometer? [Online]. Available from: https://www.researchgate.net/post/Can_we_compare_average_ roughness_values_obtained_from_AFM_and_Optical_Profilometer2/52d6cd50d2fd64580c8b45c3/citation/download. 2014, Accessed on: Sep. 10, 2020.

[16] M. Raposo, Q. Ferreira, and P. Ribeiro, “A Guide for Atomic Force Microscopy Analysis of Soft-Condensed Matter”, *Modern Research and Educational Topics in Microscopy*,” vol. 1, pp. 758-769, Jan. 2007.

[17] Nanosurf AG, Switzerland, Nanosurf FlexAFM Operating Instructions for SPM Control Software, Version 3.1, July 2012. [Online]. Available from: http://www.uel.br/proppg/portalnovo/pages /arquivos/arquivos_gerais/espec/Nanosurf%20FlexAFM%20Operating%20Instructions.pdf, Accessed on: Sep. 5, 2020.

[18] P. Klapetek, D. Neˇcas, and C. Anderson, “Gwyddion user guide,” [Online]. Available from: http://gwyddion.net/documentation /user-guide-en/, Accessed on: Sep. 4, 2020.